Early brain changes in Lyme disease are associated with clinical outcomes

Cherie L. Marvel[1,2], Alison W. Rebman[3], Kylie H. Alm[2], Pegah Touradji[4], Arnold Bakker[1,2], Prianca A. Nadkarni[1], Deeya Bhattacharya[1], Owen P. Morgan[1], Amy Mistri[1], Christopher C. Sandino[1], Jonathan A. Ecker[1], Erica A. Kozero[3], Arun Venkatesan[1], Abhay Moghekar[1], Ashar A. Keeys[1], and John N. Aucott[3]

[1]Department of Neurology, Johns Hopkins University School of Medicine, Baltimore, MD, 21205, United States of America

[2]Department of Psychiatry and Behavioral Sciences, Johns Hopkins University School of Medicine, Baltimore, MD, 21205, United States of America

[3]Division of Rheumatology, Department of Medicine, Lyme Disease Research Center, Johns Hopkins University School of Medicine, Baltimore, MD, 21205, United States of America

[4]Deparment of Physical Medicine and Rehabilitation, Johns Hopkins University School of Medicine, Baltimore, MD, 21205, United States of America

Correspondence to: Cherie L. Marvel

1501 E. Jefferson Street, Baltimore, MD 21287, USA

Cmarvel1@jhmi.edu

ORCID: 0000-0002-2818-8303

Acknowledgments

We thank Jason Creighton, Susan Joseph, and Cheryl Novak for their assistance with recruitment, screening, and data collection.

Author Contributions

The following authors contributed to the study conceptualization and design: Cherie Marvel, Alison, Rebman, Kylie Alm, Pegah Touradji, Arnold Bakker, Erica Kozero, Arun Venkatesan, Abhay Moghekar, and John Aucott. Data collection, curation, and analysis were performed by: Cherie Marvel, Alison Rebman, Kylie Alm, Pegah Touradji, Prianca Nadkarni, Deeya Bhattacharya, Owen Morgan, Amy Mistri, Erica Kozero, and Ashar Keeys. The first draft of the manuscript was written by Cherie Marvel and all authors commented on previous versions of the manuscript. All authors read and approved the final manuscript.

Abstract

In Lyme disease (LD), 10-20% of patients develop persistent symptoms following antibiotic treatment (i.e., post-treatment Lyme disease (PTLD)), which often includes neurological symptoms. This study tested the hypothesis that brain changes occur early in LD and influence outcomes.

Functional MRI (fMRI) of working memory and health surveys were administered to people with acute LD (n=20) after treatment and six months later. Demographically matched healthy controls (HC; n=19) were also assessed six months apart. The LD group was categorized at six months into those who had returned to health (RTH, n=11) or reported persistent symptoms (sPTLD, n=9). FMRI data from both LD subgroups were compared to each other and HC at both time points. Brain regions of interest (ROI) values were compared to health surveys.

Baseline brain activity in RTH was elevated in fronto-parietal regions relative to sPTLD ($p < .0025$) and HC ($p < .001$). Notably, 64% of activation clusters in RTH were in white matter, confirmed by segmentation analysis. ROI values from RTH vs. HC correlated with higher health survey scores. At 6-months, few group differences remained. By contrast, ROI values from sPTLD vs. HC yielded few activation differences at either time point or correlations with health survey scores.

Robust brain activity in early LD was associated with future RTH. By contrast, the absence of early brain activity was associated with persistent symptoms, suggesting that failure to mount an early response contributes to PTLD. Understanding how brain activity relates to recovery in LD can aid prognosis and guide treatment.

Keywords: Lyme disease, tickborne, PTLD, MRI, white matter, astrocyte

Introduction

Lyme disease (LD) is an inflammatory disease initiated by infection with *Borrelia burgdorferi* (Bb) following the bite of an infected tick. After standard of care antibiotic therapy, 10-20% of patients treated for LD will develop a chronic syndrome of patient-reported symptoms, known as post-treatment Lyme disease (PTLD). [1, 2] The Infectious Disease Society of America (IDSA)-proposed case definition of PTLD includes prior physician-documented LD, appropriate antibiotic treatment, and development of subjective complaints of fatigue, widespread musculoskeletal pain, and/or cognitive difficulties within six months of the LD diagnosis that lasts for at least six months, and results in significant social or functional decline. [3-5] Little is known about the pathophysiology of or risk factors for PTLD, and there are no FDA-approved therapeutics for curative treatment. Importantly, clinicians currently cannot identify patients who are at risk of developing PTLD at the time of acute infection. [6]

Patient-reported cognitive symptoms are common among patients with PTLD, with complaints as high as 92% of those interviewed. [6, 7] However, cognitive impairments can be associated with other illness-related factors, such as sleep disturbance, mood, fatigue, pain, and poor health-related quality of life, all of which can be significant in those with PTLD. [5] To date, few investigations *in vivo* brain studies of LD patients have been conducted, noting glial cell activity and abnormal cerebral blood flow. [8-10] Recently, PTLD and healthy control participants performed a cognitive task while undergoing functional MRI (fMRI). [11] In the PTLD group relative to controls, white matter activations were observed, a phenomenon which is highly unusual. [12-14] Moreover, imaging characteristics within these white matter activations correlated with *fewer* cognitive and neurological symptoms. Thus, evidence suggests that the brain can be altered by LD, these alterations involve white matter, and, perhaps counterintuitively, such changes are associated with better clinical outcomes.

The current case-control study examined brain changes associated with early LD within weeks of the first diagnosis of acute infection and again six months later to capture the onset of white matter changes in LD. We hypothesized that white matter changes would emerge within the first six months post-infection and would be associated with favorable clinical outcomes, consistent with prior findings in a cross-sectional PTLD cohort. [11]

Materials and methods

Participants

Adults with LD were recruited from the Johns Hopkins Lyme Disease Research Center in which they were enrolled in the on-going Study of Lyme Immunology and Clinical Events (SLICE). [15] For SLICE enrollment, participants were required to have a visible, diagnostic erythema migrans rash ≥ 5 cm and to not have been ill longer than 3 months. Patients were excluded if they self-reported a medical history of any conditions with significant symptom overlap with PTLD, similar to those listed in the IDSA's proposed case definition. [3] Specifically, those with fibromyalgia, chronic fatigue, major immunosuppression, psychiatric or autoimmune illnesses, hepatitis B/C, HIV, cancer chemotherapy treatment in the past two years, a history of illicit drug or substance abuse, Long COVID, or current pregnancy were excluded.

Healthy controls (HC) were recruited via community flyers and screened for any co-morbid conditions with significant symptom overlap with PTLD, as well as the exclusion criteria described above, or a past diagnosis of LD.

In a final screening stage, both LD and HC participants were excluded from study participation if they endorsed the following characteristics that might confound data interpretation: history of major neurologic disorders (including history of stroke, seizures, or HIV); a prior head injury resulting in loss of consciousness for longer than 5 minutes; current severe or unstable medical disorder; history before LD of a significant learning disability; and history before LD of a severe mood or psychotic disorder. Participants were also excluded for contraindications within the MRI environment, such as surgical implants and claustrophobia. Finally, participants were excluded for left-handedness or being a non-native English speaker (unless English was learned before puberty) because each of these would confound results due to the nature of the verbal working memory task administered during fMRI.

Participants were asked to return six months after their MRI to re-assess clinical and cognitive variables, obtain a second MRI, and determine health outcomes post infection. Data were removed from analyses if a participant dropped out of the SLICE study before an outcome could be ascertained, fMRI data was unusable, or there was an incidental MRI finding. In some cases, participants did not return for their follow-up MRI, but remained in the SLICE study, enabling a health outcome determination, and their baseline data were included.

The Institutional Review Board of the Johns Hopkins University School of Medicine approved this study. Written informed consent was obtained according to the Declaration of Helsinki

from all participants prior to initiation of study activities, and all participants received compensation.

Clinical assessment

Overall health, mood, symptom severity, fatigue, pain and health-related quality of life were assessed by standardized questionnaires which were administered at the baseline and 6-month visits: Short Form Health Survey, version 2 (SF-36) [16], Fatigue Severity Scale (FSS) [17], Short-Form McGill Pain Questionnaire-2 (SF-MPQ-2) [18], Beck Depression Inventory II (BDI-II) [19], and a self-administered a 36-item measure of symptom presence and severity (the post-Lyme Questionnaire of Symptoms [PLQS]). [20] For questionnaires, higher scores indicated greater symptom severity, except on the SF-36 where higher scores indicated higher health-related quality of life and functioning. (Online Table1)

Patient outcome status was determined at the 6-month follow-up visit. Due to the relatively small sample size, we dichotomized patients into two groups only; those who met criteria for return to health (RTH) vs. all others, who were considered sPTLD with either symptoms and/or functional impact present. [20, 21] Patients met criteria for RTH if: a) their PLQS did not indicate the presence of either fatigue, musculoskeletal pain, or cognitive complaints at the 'moderate' or 'severe' level, and b) their average composite score of 4 specific norm-based subscales on the SF-36 was no greater than 0.5 SD below the population mean. [21] Remaining patients not meeting criteria for RTH were considered sPTLD with either symptoms and/or functional impact present.

Cognitive assessment

Standardized cognitive tests were administered at each timepoint. (see Online Table 2 for a list of tests) Raw scores were converted to T-scores using established norms.

fMRI tasks

Verbal working memory task

Participants performed a verbal working memory task in the MRI scanner that has been described previously. [11, 22, 23] The paradigm involved two task conditions, each consisting of two stimulus conditions, resulting in four overall study conditions. Briefly, in the "control" condition, participants visually encoded one or two letters, and after a 4-6 second delay, they indicated by button press whether a probe letter matched a target letter. In the "forward"

condition, participants again visually encoded one or two letters. During the delay period, however, they counted two alphabetical letters forward of each letter and held those new letters in mind. For example, if the letters were ‘‘f” and ‘‘q”, participants would hold ‘‘h” and ‘‘s” in mind. When the probe letter appeared, participants indicated whether the probe matched the newly derived target letters. Thus, there were four conditions total: 1) one-letter control, 2) two-letters control, 3) one-letter forward, and 4) two-letters forward. Additional parameter details are provided in Online Methods1. The measures of interest were accuracy and response time (RT) for each condition, with no minimal performance threshold for data inclusion. Due to a technical error, responses from one control participant were not recorded. This participant was not included in the behavioral analysis but remained in the fMRI analysis by including all trials.

Hemodynamic response function (HRF) tapping task

Individualized HRFs were obtained for convolutions during the event-related fMRI analyses to account for potential HRF differences across participants or study groups. This was obtained via a tapping task involving the right index finger. Tapping blocks lasted ~30 seconds upon presentation of “tap” instructions, followed by “rest”, also lasting ~ 30 seconds, for a total duration of 10 minutes. [11, 22, 24, 25]

MRI data acquisition

All MRI data were acquired on a Philips 3 Tesla scanner using a 32-channel head coil. Equipment information is detailed in Online Methods2.

Structural MRI

A sagittal magnetization prepared gradient-echo (MPRAGE) sequence aligned to the anterior-posterior commissure (AC-PC) axis was used with the following parameters: repetition time (TR)/echo time (TE) = 7/3.3 ms; field of view = 240 mm x 240 mm; 170 slices; slice thickness 1.0 mm; 0 mm gap; flip angle = 8 degrees; voxel size = 0.75 mm x 0.75 mm. The total scan duration was 6 minutes.

Functional MRI

A T2-weighted gradient echo EPI pulse sequence was used with the following parameters: TR = 1000 ms; TE = 30 ms; flip angle = 61 degrees; in-plane resolution = 3.75 mm; slice thickness = 6 mm with a 1 mm gap; 20 oblique-axial slices; FOV = 21mm x 240 mm. To maximize

whole-brain coverage to include the cerebellum and neocortex, images were acquired in the oblique-axial plane rotated 25 degrees clockwise with respect to the AC-PC line. The number of acquired volumes within each run ranged from 917 to 922 for the working memory tasks and 630 for the tapping task. The start of the fMRI scan was triggered by Eprime 2.0 software (Psychology Software Tools, Pittsburgh, PA) at the beginning of each run.

MRI data analysis

Functional data analysis

Standard image preprocessing steps were performed using SPM12 [26]: slice timing correction (reference = slice #10), motion correction of all volumes aligned to the first volume of the first run, anatomical co-registration, normalization to the Montreal Neurological Institute (MNI) stereotaxic space, and spatial smoothing (FWHM = 8 mm). Individual HRF regressors were convolved with reference waveforms for the delay phase of the task (i.e., the 4-6 second delay between target and probe presentation) for each participant within the first-level analysis. This represented an event-related analysis focusing on working memory in the absence of visual stimuli or motor response. Statistical maps were computed for each participant using the general linear model approach with high pass filtering of 128 seconds. A random effects analysis was performed to map the average responses for correct trials only. All trials were included for one control at baseline whose behavioral data was not recorded due to a technical error. A beta contrast volume per participant was computed and used to conduct one-sample t-test values at every voxel. Within-group contrasts compared the blood oxygen level dependence (BOLD) signal difference between the two-letters forward minus two-letters control conditions. These differences were compared between group pairs (i.e., All Lyme vs. HC, RTH vs. HC, sPTLD vs. HC, and RTH vs. sPTLD). Activations were identified using a threshold of $p < .001$ with a cluster-level $k \geq 10$. ROIs were created from surviving clusters using the Mars-BaR toolbox for SPM. [27] Individual ROI values were segmented for tissue classification. ROIs containing > 50% white matter were considered white matter activations. Gray and white matter activations were correlated with cognitive and clinical variables. For anatomical determinations of the activations, MNI coordinates were transformed into the coordinate system of the Talairach and Tourneaux stereotaxic atlas [28] using Bioimage Suite Web (Version 1.2.0) [29] and cross-referenced with atlas manuals. [28, 30]

Tissue class segmentation analysis

Following methods developed previously [11], significant fMRI activation clusters for each contrast and timepoint of interest were first transformed into binary ROIs masks, and then resampled into 1 mm^3 space using nearest neighbor interpolation to match the MPRAGE template space used for tissue class segmentation. A study-specific T1 modal model template was generated using all participants and both timepoints. Advanced Normalization Tools (ANTs) software [31, 32] was used to calculate a 3D vector field transformation for each MPRAGE image input aligned to the study-specific template space. FSL's FAST automated segmentation [33, 34] was used to segment the template into three tissue classes: gray matter, white matter, and cerebrospinal fluid. Each binary ROI mask was multiplied by the binary white matter segmentation mask, yielding the number of white matter voxels per ROI. This value was divided by the number of voxels in the entire ROI and multiplied by 100 to yield the percentage of white matter voxels. ROIs that contained > 50% white matter were categorized as "white matter activations" in subsequent analyses.

ROI analysis with clinical & cognitive variables

The estimate of activation within gray and white matter clusters were computed using Mars-BaR. [27] All voxel values within the ROI were averaged to yield one value per ROI. This value was correlated to variables obtained from questionnaires and cognitive tests.

Statistical analysis

The clinical, cognitive, and MRI data contained continuous variables, except gender, which was categorical. In group comparisons (RTH vs. sPTLD, RTH vs. HC, and sPTLD vs. HC), t-tests and one-way ANOVA tests were used to compare continuous variables (e.g., age and education), and Fisher's Exact test was used to compare gender. P-values for t-tests were determined by the result of the Levene's Test for Equality of Variances. Shapiro-Wilk tests were used to determine if continuous variables followed a normal distribution. If a variable was not normally distributed, Mann-Whitney U-tests and Kruskal-Wallis tests were conducted to compare groups. Mixed-design ANOVAs were used to compare repeated measures between groups (e.g., fMRI task performance). [No ANOVAs contained a within-subjects factor with more than two levels; sphericity corrections were, therefore, not needed.] If mixed-design ANOVAs revealed group effects, pairwise t-tests were conducted to determine which groups were affected differentially. Pearson correlations were used when the Shapiro-Wilk's

normality tests indicated a normal data distribution (e.g., correlating ROI values with symptom measures). Spearman's rho nonparametric correlations were used for variables with non-normal data distributions. However, ROI values were correlated to clinical and cognitive scores using Spearman's correlations in all cases for a conservative approach in the absence of correction for multiple comparisons. Missing data within a symptom rating scale was imputed such that the mean for all other symptom items for an individual was entered as the missing value and fed into the summary score. All tests were two-tailed, with an alpha level < .05 to define statistical significance. Statistics were performed using IBM SPSS Statistics, Macintosh, version 29 (IBM Corp., Armonk, NY, USA).

Results

Participants

Adults with early LD (n=23) and HC (n=21) consented for this study between 2017-2022. A final sample of 20 LD participants were included in the baseline and 17 in the follow-up analysis; 19 HC participants were included in the baseline and 16 in the follow-up analysis (Fig. 1). LD participants completed their baseline fMRI visit with a mean of 15.2 days (range: 1-51) after completing doxycycline treatment and a mean of 42.3 days (range: 25-79) after the onset of their LD.

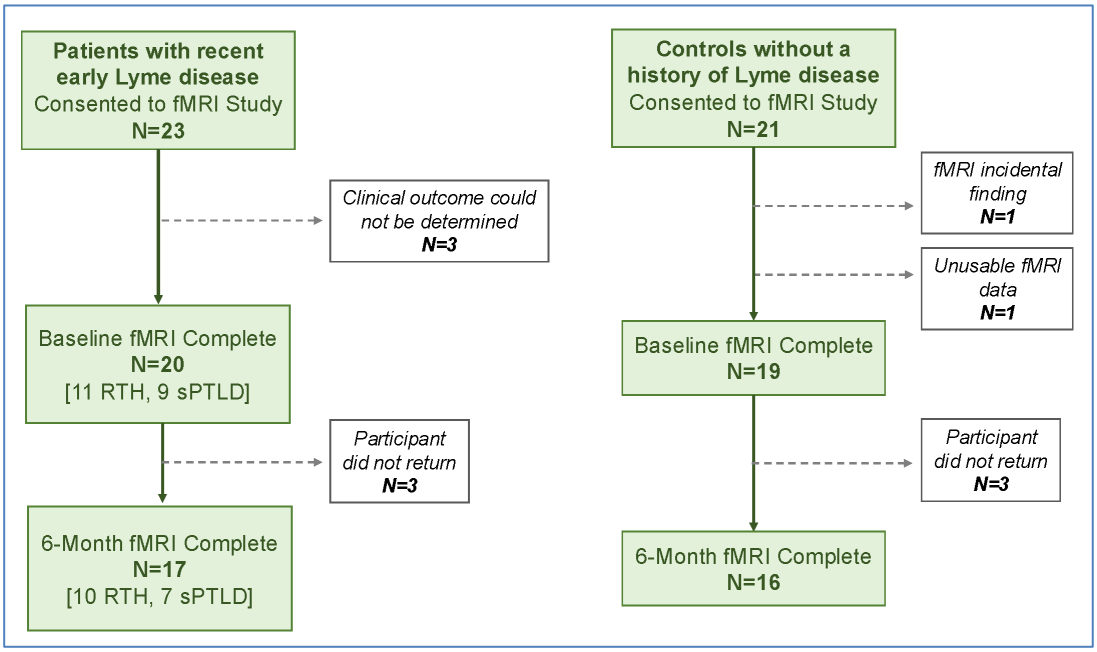

Fig. 1 Study recruitment and retention data. Description of sample sizes for both study groups from consent to completion

Based on clinical and health measures obtained at six months, 11 Lyme participants were assigned to the RTH group and nine to the sPTLD group. (Table 1) Groups (sPTLD, RTH, and HC) did not differ by age *(H(2) = 3.02, p = .221*), years of education ($F(2,36) = .042$, $p = .959$), or gender, $p = .214$. Comparisons between the RTH and sPTLD groups revealed no differences in the median days' duration between LD onset and receiving antibiotic treatment (RTH = 4.00 vs. sPTLD = 6.00, $U = 46.0$, $p = .819$), between LD onset and receiving the first MRI scan (RTH = 36.00 vs. sPTLD = 38.00, $U = 56.5$, $p = .603$), or between ending antibiotics and receiving the first MRI scan (RTH = 10.00 vs. sPTLD = 12.00, $U = 56.5$, $p = .603$). Groups did not differ in the duration between MRI scans ($H(2) = .530$, $p = .767$).

Table 1 Baseline demographic and clinical characteristics

	RTH (*n*=11)	**sPTLD (*n*=9)**	**HC (*n*=19)**
Age (years)	56.51 (14.57)	47.14 (14.72)	51.16 [37.47, 57.93]
Male Gender	5 (45.45%)	6 (66.67%)	6 (31.58%)
Education (Years)	16.55 (2.62)	16.78 (2.22)	16.53 (1.98)
Two-Tier Seropositive[1]	5/10[1] (50.00%)	6 (66.67%)	0 (0.00%)
Disseminated EM Lesions[2]	6 (54.44%)	3 (33.33%)	N/A
Lyme Disease Duration Prior to Treatment (Days)	6.59 (4.85)	6.00 [3.00, 6.00]	N/A
Lyme Disease Duration at first fMRI (Days)	36.00 [31.00, 52.00]	40.89 (8.49)	N/A
Days Since Stopping Doxycycline at First Scan (Days)[3]	10.00 [4.00, 26.00]	13.0 (4.97)	N/A
Days Between MRI Scans[4]	192.00 (18.28), n=10	199.14 (23.57), n=7	184.50 [179.50, 201.50], n=16

N (%) are presented for categorical variables. Mean (standard deviation) are presented for normally distributed continuous variables, and median [IQR] are presented for non-normally distributed continuous variables. Sample sizes are presented when missing data occurred. No group differences were found across variables, all p-values > .214.
[1]Based on acute and convalescent testing interpreted according to CDC criteria which account for illness duration at the time of the test. One RTH patient was missing complete serostatus information.
[2]No patients had early disseminated neurologic or cardiac Lyme disease at the time of diagnosis.
[3]One person was at the end of their doxycycline treatment when the first scan was performed.
[4] One RTH, two sPTLD, and three HC participants did not return for their 6-month MRI scan.

Clinical assessment

At baseline, the patient groups differed on the SF-36 (Social Functioning Scale, $U = 18.00$, $p = .033$; Mental Component Scale, $t(17) = 2.86$, $p = .011$) and the PLQS (Symptoms Total, $U = 68.50$, $p = .041$). At follow-up, patient groups differed on the BDI Total, $U = 11.00$, $p = .023$; the BDI Cognitive/Affective Subscale, $U = 13.00$, $p = .039$, and the PLQS (Symptoms Total, $U = 8.00$, $p = .003$). (Table 2)

Table 2 Standardized symptom measures

		Baseline Visit		**6-Month Follow-up**	
		RTH	**sPTLD**	**RTH**	**sPTLD**

	n=11	*n*=9	*n*=10	*n*=7
Beck Depression Inventory-II Total	4.82 (3.76)	9.43 (7.91), n=7	.00 [.00, 3.00], n=9*	6.57 (6.58)*
Beck Depression Inventory-II Cognitive/Affective Subscale	1.00 [.00, 3.00]	4.29 (3.90), n=7	.00 [.00, 0.00], n=9*	4.00 (5.00)*
Beck Depression Inventory-II Somatic Subscale	2.82 (1.83)	5.14 (4.41), n=7	.00 [.00, 1.00], n=9	2.57 (2.07)
SF-36 Mental Health	57.95 (4.33)	46.84 (14.16), n=8	58.46 [55.64, 58.46]	52.83 (9.34)
SF-36 Role Emotional	55.88 [51.99, 55.88]	53.94 [32.56, 55.88], n=8	55.88 [55.88, 55.88]	55.88 [36.44, 55.88]
SF-36 Social Functioning	56.85 [45.94, 56.85]*	37.76 (15.97), n=8*	56.85 [56.85, 56.85]	45.94 [45.94, 56.85]
SF-36 Vitality	51.24 (9.78)	42.33 (15.87), n=8	58.33 [58.33, 61.46]	52.09 (11.40)
SF-36 General Health	53.00 (8.73)	51.03 (7.81), n=8	57.23, [55.32, 62.47]	52.46 (6.34)
SF-36 Bodily Pain	52.17 (8.12)	43.68 (15.33), n=8	55.36 [55.36, 55.36]	53.49 (8.61)
SF-36 Role Physical	49.28 (6.97)	40.63 (15.54), n=8	56.85 [54.40, 56.85]	50.55 (7.46)
SF-36 Physical Functioning	51.77 [42.30, 57.03]	52.82 [43.55, 55.98], n=8	54.93 [50.72, 57.03]	54.93 [50.72, 57.03]
SF-36 Mental Component	56.87 (5.41)*	42.60 (15.44), n=8*	56.90 [56.10, 58.19]	49.69 (10.84)
SF-36 Physical Component	47.80 (9.25)	46.37 (11.02), n=8	56.16 [55.08, 57.48]	53.30 (3.35)
Post-Lyme Questionnaire of Symptoms Total	1.00 [.00, 1.00]*	3.00 [1.00, 5.50], n=8*	.00 [.00, 1.00]*	2.00 [1.00, 6.00]*
Post-Lyme Questionnaire of Symptoms Cognitive Subscale	0.00 (0.00)	.00 [.00, 1.00], n=8	.00 [.00, 1.00]	.00 [.00, .00]
Post-Lyme Questionnaire of Symptoms Neuro Subscale	.00 [.00, 1.00]	1.75 (2.05), n=8	.00 [.00, .00]	1.00 [.00, 2.00]
Fatigue Severity Scale Total	23.80 (12.44), n=10	34.13 (21.82), n=8	19.30 (9.37)	22.71 (12.87)
Short Form McGill Pain Questionnaire Total	1.00 [.00, 2.00], n=10	3.38 (4.17), n=8	0.50 [.00, 2.00]	3.57 (4.43)
Short Form McGill Pain Questionnaire Affective Subscale	.00 [.00, 1.00], n=10	.00 [.00, 1.50], n=8	.00 [.00, .00]	0.00 [0.00, 0.00]
Short Form McGill Pain Questionnaire Sensory Subscale	.50 [.00, 1.00], n=10	2.63 (3.29), n=8	0.50 [.00, 2.00]	3.43 (4.12)

Mean (standard deviation) are presented for normally distributed continuous variables, and median [IQR] are presented for non-normally distributed continuous variables.
Sample n's are presented for any measures with missing data.
Significant group differences are marked for each test '*' = sPTLD vs. RTH, $p < .05$.

Cognitive assessment

At baseline, the HC group scored higher than the RTH and sPTLD groups on Trails A, (vs. RTH: $t(28) = 2.17, p = .038$; vs. sPTLD: $t(26) = 2.49, p = .019$). At follow-up, HC and patient groups showed no significant differences. The RTH vs. sPTLD groups showed no significant differences at either timepoint. (Online Table3)

Tests were run to identify changes in cognitive test performance between the two timepoints. A 2(timepoint: baseline vs. follow-up) by 3(group: HC vs. sPTLD vs. RTH) mixed-design ANOVA was run for each cognitive test that was administered. A main effect of timepoint was observed for the Digit Span test $(F(1, 30) = 4.76, p = .037)$ and Trails A test $(F(1, 29) = 7.50, p = .010)$, with all groups improving on both tests. There also was a main effect of group for

the Trails A test *(F(1, 29) = 4.28, p = .024*). Post-hoc pairwise t-tests for Trails A indicated that the HC group's improvement across visits was marginally significant, *t(15) = -2.04, p = .060*). By contrast, the patient groups showed no improvement across visits, (sPTLD: *t(5) = -1.26, p = .263*; RTH: *t(9) = -1.53, p = .160).*

fMRI verbal working memory task

Mean accuracy and RT (for accurate trials only) were computed for the forward and control tasks at each timepoint. A 2(condition: control vs. forward) x 2(stimulus type: 1 vs. 2) x 3(group: HC vs. sPTLD vs. RTH) mixed-design ANOVA was conducted for the participants' mean accuracy scores at the baseline visit. At baseline, there was an interaction of condition by stimulus type *(F(1, 35) = 7.78, p = .008),* which remained at follow-up *(F(1, 29) = 6.00, p = .021).* There were no significant effects of group on the mean accuracy at either timepoint. As shown in Online Table3, the condition by stimulus type interactions were due to reduced accuracy on the two-letters forward condition.

The same 2x2x3 mixed-design ANOVA was conducted for the mean RTs at each timepoint. At the baseline visit and at follow-up, there were interactions of condition by stimulus type *(F(1, 34) = 22.7, p < .001) and (F(1, 29) = 20.8, p < .001),* respectively. There were no significant effects of group on the mean RTs at either timepoint. As with the accuracy data, the condition by stimulus type interactions were due to increased RTs on the two-letters forward condition. Due to the disproportionate difficulty experienced by both groups on the two-letters forward condition, fMRI analyses focused on results obtained from this condition.

MRI data

BOLD signal activations were compared between groups in a double subtraction approach: within-group contrast values for "two-letters forward" minus "two-letters control" conditions were obtained (first subtraction), then these values were compared between groups (second subtraction).

All Lyme vs. HC

At baseline, between-groups analysis revealed eight activations; all were in the direction of All Lyme participants showing elevated activation compared to HC. (Table 3) Strikingly, six of the eight activations (75%) were located in white matter, within the frontal lobe, temporal lobe, and cerebellum. With many areas of activation located in white matter, the observed brain circuitry did not align with prior reports using this fMRI task. [11, 22, 35] At 6-month follow-

up, group differences revealed only two areas of activation, both in the direction of Lyme participants showing elevated activation compared to HC, and both located in the frontal lobe (one was in white matter).

Table 3 FMRI activation differences during the fMRI working memory task at baseline and 6-month follow-up.

Cluster size (voxels)	T-value	X, Y, Z (MNI)	Brain Region (BA)	% White Matter
Baseline Regions of Activation				
All Lyme > HC				
67	4.31	-42, -22, -8	L Temporal Lobe	**91***
36	4.25	-16, -12, 36	L Frontal Lobe	**100**
65	4.04	-36, -16, 54	L Frontal Lobe	**56***
54	4.03	12, -22, 68	R Frontal superior gyrus (BA 6)	47*
26	3.83	-32, 4, 36	L Frontal Lobe	**95**
31	3.68	-16, -48, -28	L Cerebellar Anterior Lobe	**97**
11	3.66	-50, 18, 18	L Frontal Lobe	**61**
21	3.58	2, -72, -36	R Cerebellar Vermis VIIB	9
HC > All Lyme				
None				
RTH > HC				
134	5.45	-16, -12, 38	L Frontal Lobe	**97***
217	5.01	-34, -18, 54	L Frontal Lobe	**52***
190	4.77	12, -22, 68	R Superior frontal gyrus (BA 6)	41*
191	4.60	46, -8, 32	R Precentral Gyrus (BA 6)	41*
63	4.33	-42, -22, -8	L Temporal Lobe	**87***
198	4.19	-30, 4, 36	L Frontal Lobe	**78***
152	4.00	30, -44, 24	R Parietal Lobe	**99***
64	3.98	2, -72, -32	R Cerebellar Vermis VIIB	12*
26	3.97	-8, -20, 70	L Frontal Lobe	**84**
81	3.94	62, -8, 12	R Postcentral Gyrus (BA 43)	32*
32	3.92	-22, -56, 36	L Parietal Lobe	**100**
15	3.81	-24, 22, 20	L Frontal Lobe	**100**
10	3.78	36, -10, -20	R Hippocampus	20
26	3.77	-34, -36, 26	L Parietal Lobe	**99**
HC > RTH				
None				
sPTLD > HC				
25	4.37	-4, -40, -18	L Cerebellar Lobule III	29
HC > sPTLD				
None				
RTH > sPTLD				
78	4.13	48, -10, 32	R Post Central Gyrus (BA 4)	9*

10	3.93	-18, -12, 40	L Frontal Lobe	**100**
34	3.93	-52, 24, 8	L Inferior Frontal Gyrus (BA 45)	30^
11	3.71	-14, -60, 48	L Parietal Lobe	**88^**
36	3.58	38, -46, 20	R Parietal Lobe	**95^**
12	3.42	16, -4, 48	R Frontal Lobe	**74^**
sPTLD > RTH				
None				
6-Month Follow-up Regions of Activation				
All Lyme > HC				
32	4.38	-28, 10, 60	L Middle Frontal Gyrus (BA 6)	4
10	4.02	34, 34, 6	R Frontal Lobe	**96**
HC > All Lyme				
None				
RTH > HC				
17	4.60	34, 32, 6	R Frontal Lobe	**78**
10	3.86	-28, 10, 58	L Middle Frontal Gyrus (BA 6)	1
HC > RTH				
None				
sPTLD > HC				
50	5.81	-30, 10, 62	L Middle Frontal Gyrus (BA 6)	8
HC > sPTLD				
None				
RTH > sPTLD				
15	4.57	42, -80, 18	R Occipital Lobe	**56**
19	4.06	20, -64, 32	R Precuneus (BA 7)	7^
52	3.80	44, -14, 36	R Post Central Gyrus (BA 4)	19^
41	3.77	62, -4, 16	R Post Central Gyrus (BA 4)	16^
10	3.62	-14, -48, -40	L Cerebellar Lobule IX	48^
21	3.58	-24, -44, 34	L Parietal Lobe	**88^**
sPTLD > RTH				
13	4.34	-56, 20, 14	L Inferior Frontal Gyrus (BA 45)	0
17	4.30	58, 20, 20	R Inferior Frontal Gyrus (BA 45)	15

Primary threshold = p <.001 and k ≥ 10; ^ threshold = p < .0025 and k ≥ 10.
MNI = Montreal Neurological Institute coordinates; BA = Brodmann Area.
Bold % white matter indicates > 50%.
For white matter > 50%, the brain region was reported within the relevant lobe.
* indicates the activation passed p < .001 and also surpassed k ≥ expected voxels per cluster (i.e., beyond k≥ 10 voxels)

RTH vs. HC

At baseline, between-groups analysis yielded 14 activations, all in the direction of RTH showing elevated activation compared to HC. Of these, nine (64%) were in white matter. At follow-up, group differences revealed two activations, both in the direction of RTH showing elevated activation than HC and located in the frontal lobe (one was in white matter). (Fig. 2)

Activation patterns at both time points closely resembled those observed in the All Lyme vs. HC comparisons, suggesting that the RTH group drove the All Lyme vs. HC results.

sPTLD vs. HC

At baseline, between-groups analysis revealed one gray matter activation in the cerebellum, in the direction of sPTLD showing elevated activation compared to HC. At follow-up, group differences revealed one gray matter activation in the frontal lobe, reflecting elevated activation in sPTLD compared to HC. (Fig. 2)

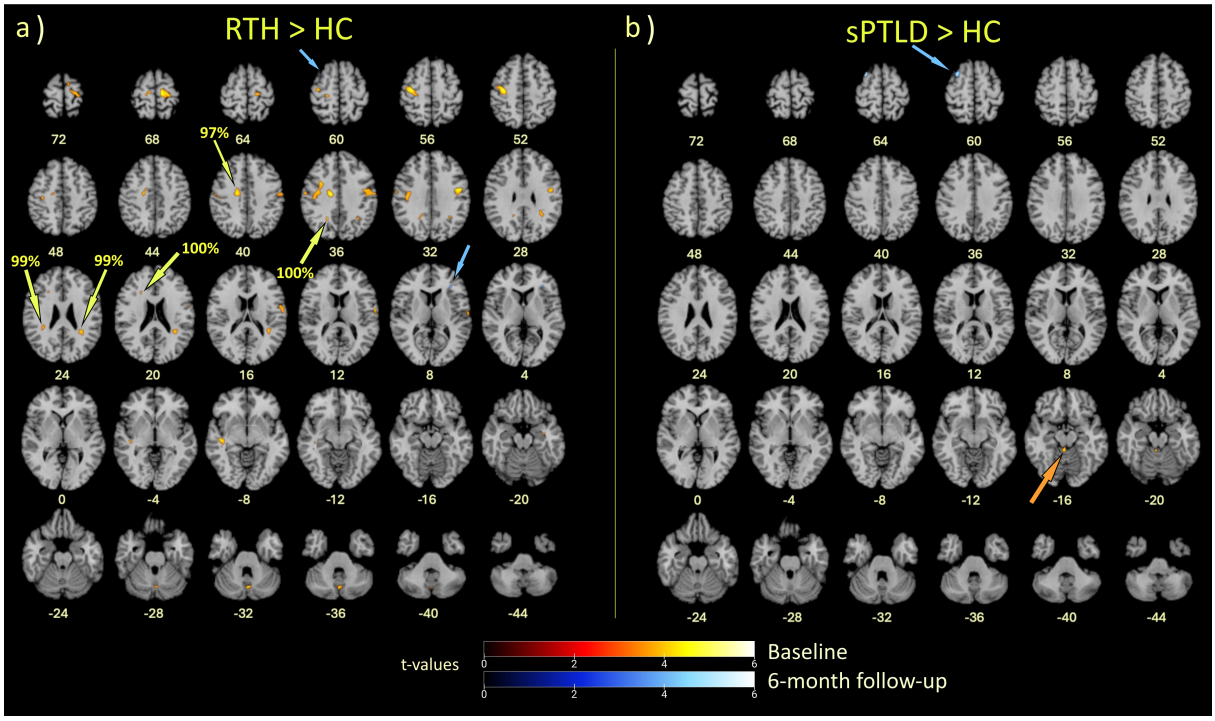

Fig. 2 fMRI cluster overlays representing between-group activation differences during baseline and follow-up scans. a) RTH > HC: Numerous activation differences were evident at baseline (red-yellow spectrum clusters). Clusters that were > 90% white matter are denoted by the yellow arrows. Only two activation differences were observed six months later (blue spectrum clusters; blue arrows). **b)** sPTLD > HC: One activation difference at baseline and at 6-month follow-up were observed, indicated by orange and blue arrows, respectively. Cross-reference with Table 3 for cluster information. Scale shows t-values 0 – 6. Images are shown in neurological convention with right side on the right. Threshold = $p < .001$ and $k \geq 10$.

RTH vs. sPTLD

At baseline, between-groups analysis revealed two activations, with RTH showing elevated activation compared to sPTLD. One activation was located in white matter, and both were in the frontal lobe. At follow-up, group differences revealed one area of elevated activation in occipital lobe white matter of RTH compared sPTLD. We expected to see more group

differences in the direction of RTH stronger than sPTLD, given each subgroup's results compared to HC. Therefore, we explored direct subgroup comparisons using a slightly more liberal threshold of $p < .0025$, $k \geq 10$. Indeed, this revealed four additional activations at baseline, all with the RTH group showing stronger activations than the sPTLD group (three in white matter). At six months, five additional activations were revealed in favor of the RTH group showing stronger activations (one in white matter). (Table 3)

Longitudinal Comparisons

Within-group analyses compared activations at baseline and follow-up, but no suprathreshold clusters were revealed.

Tissue class segmentation results

At baseline, 75% of ROIs were located in white matter for All Lyme vs. HC. When RTH vs. HC was examined separately from sPTLD vs. HC, 64% of the ROIs were located in white matter, thereby driving the All Lyme vs. HC results. At the 6-month follow-up, there was a reduction in group brain activity differences, with the All Lyme vs. HC and RTH vs. HC comparisons nearly identical, each revealing two ROIs, with one of them in white matter. No white matter activations were observed in the sPTLD group at either timepoint.

Relationship between fMRI and clinical and cognitive scores

For clinical correlates, baseline activation signals from the ROIs in the RTH group generally correlated with better clinical outcomes, regardless of whether the ROIs were found in gray or white matter. (Fig. 3) Six months later, this relationship had reversed. ROI activity generally correlated with patients feeling worse in the RTH group. By contrast, in the sPTLD group at baseline, ROI activity generally associated with poorer clinical outcomes. Six months later, this relationship had dissipated without a clear association between brain activity and clinical outcomes.

		Regions of Activation	Health Surveys													
			SF-36										PLQS Total Number	BDI Total Score	Fatigue Severity Scale Total	McGill Pain Total Score
			Mental Component	Mental Health	Role Emotional	Social Function	Vitality	General Health	Bodily Pain	Role Physical	Physical Function	Physical Component				
			Baseline Visit													
RTH > HC	WM	*L Frontal Lobe (-16, -12, 38)*	0.673	0.280	0.250	**0.657***	**0.618***	0.378	0.381	0.380	0.175	0.173	**-0.655***	0.432	**-0.663***	-0.489
		L Parietal Lobe (-22, -56, 36)	-0.173	-0.187	0.615	0.311	0.249	**0.633***	0.237	0.472	0.569	**0.664***	-0.201	-0.178	0.000	0.127
		L Frontal Lobe (-24, 22, 20)	0.600	0.439	0.708	**0.708***	0.548	0.469	0.353	0.167	0.450	0.364	-0.445	0.322	-0.401	-0.693
		L Frontal Lobe (-30, 4, 36)	0.273	-0.150	0.400	0.454	0.433	0.551	0.274	0.500	0.238	0.336	-0.347	0.110	-0.571	-0.114
		L Frontal Lobe (-34, -18, 54)	0.173	-0.154	0.325	0.392	0.396	**0.624***	0.255	0.352	0.288	0.336	-0.215	0.226	-0.602	0.102
		L Parietal Lobe (-34, -36, 26)	0.291	0.173	0.708	**0.612***	0.530	**0.738***	0.487	0.380	0.663	0.673	-0.401	0.034	-0.231	-0.369
		L Temporal Lobe (-42, -22, -8)	0.573	0.229	0.383	**0.749***	0.461	0.164	0.111	0.259	-0.019	-0.009	-0.523	0.432	-0.456	-0.089
		L Frontal Lobe (-8, -20, 70)	0.273	-0.159	0.209	0.418	0.318	0.478	0.060	0.426	-0.088	0.073	-0.391	0.350	**-0.711***	0.369
		L Parietal Lobe (30, -44, 24)	0.136	-0.182	0.574	0.591	0.277	0.246	0.274	0.259	0.244	0.373	-0.303	-0.089	-0.134	-0.280
	GM	*R Superior Frontal Gyrus (BA 6) (12, -22, 68)*	0.373	-0.042	0.342	**0.652***	0.415	0.337	0.149	0.435	-0.006	0.100	-0.347	0.219	-0.450	0.273
		R Cerebellar Vernis VIIB (2, -72, 32)	0.109	0.075	0.749	0.494	0.189	0.355	0.060	0.148	0.306	0.373	-0.367	0.171	-0.122	-0.127
		R Hippocampus (36, -10, -20)	0.336	0.196	0.540	**0.627***	0.507	0.442	0.232	0.278	0.444	0.373	-0.567	0.452	-0.419	-0.248
		R Precentral Gyrus (BA 6) (46, -9, 32)	0.191	-0.070	0.592	0.357	0.267	**0.610***	0.079	0.352	0.206	0.327	-0.357	0.199	-0.584	-0.044
		R Postcentral Gyrus (BA 43) (62, -8, 12)	0.573	0.369	0.650	0.612	0.475	0.538	0.158	0.306	0.244	0.255	**-0.621***	0.452	-0.614	-0.375
sPTLD > HC	GM	*L Cerebellar Lobule III (4, -40, -18)*	-0.429	-0.293	-0.575	-0.386	-0.422	-0.168	-0.096	-0.371	-0.675	-0.405	0.374	0.050	0.168	0.712*
			6 Month Follow-Up Visit													
RTH > HC	WM	*R Frontal Lobe (34, 32, 6)*	0.345	0.274	0.000	-0.174	-0.551	-0.412	-0.206	-0.206	-0.559	-0.648*	0.266	-0.020	0.042	0.610
	GM	*L Middle Frontal Gyrus (BA 6) (-28, 10, 58)*	0.152	0.247	-0.435	-0.522	-0.506	-0.326	-0.295	-0.308	-0.445	-0.442	-0.266	-0.269	0.515	**0.662***
sPTLD > HC	GM	*L Middle Frontal Gyrus (BA 6) (-30, 10, 62)*	0.000	0.180	-0.079	0.424	0.164	-0.468	0.505	0.482	0.265	0.714	0.270	-0.357	0.432	0.000

Fig. 3 Correlation matrix for ROI values and clinical assessment scores. Shades of red = positive correlation direction; shades of blue = negative correlation direction. Note that the SF-36 uses an inverse relationship to severity of illness. Correlations were run using Spearman's rank; significance is denoted by * <.05 if correlations also passed visual scatterplot inspection.

At the baseline visit, correlations between ROI values and cognitive scores did not show clear associations for either group. (Fig. 4) At follow-up, however, the sPTLD group skewed towards negative associations between brain activity and cognitive function, with significant correlates for assessments of processing speed and executive function (Digit Symbol Coding and Trails B). Negative correlates on additional tests (HVLT Total, Trails A, and COWA) were also quite strong, with $r_s > .6$, which did not meet the threshold using non-parametric testing, but were consistent with difficulties in processing speed, attention, and language functions.

		Regions of Activation	Cognitive Tasks										
			WRAT	Digit Span	Coding	HVLT Total	HVLT Delayed	Trails A	Trails B	fMRI Accuracy	fMRI Reaction Time	FAS COWAT	Animals COWAT
			Baseline Visit										
RTH > HC	WM	*L Frontal Lobe (-16, -12, 38)*	-0.338	-0.149	-0.204	**0.680***	0.253	-0.255	-0.037	-0.195	-0.309	-0.317	-0.212
		L Parietal Lobe (-22, -56, 36)	0.174	-0.009	0.370	-0.251	-0.248	0.005	-0.266	0.157	0.127	-0.305	0.067
		L Frontal Lobe (-24, 22, 20)	-0.119	-0.265	-0.324	0.247	-0.175	-0.588	-0.248	-0.271	0.006	-0.274	0.139
		L Frontal Lobe (-30, 4, 36)	-0.132	0.074	0.398	0.434	0.382	-0.018	0.009	0.245	-0.418	-0.091	0.055
		L Frontal Lobe (-34, -18, 54)	0.100	0.293	0.185	0.219	0.074	-0.105	0.018	0.183	-0.321	0.006	0.261
		L Parietal Lobe (-34, -36, 26)	0.169	-0.060	0.083	-0.041	-0.271	-0.469	-0.229	-0.220	0.152	-0.122	0.297
		L Temporal Lobe (-42, -22, -8)	-0.187	-0.070	-0.296	0.347	-0.244	-0.087	-0.193	0.000	-0.079	-0.213	0.042
		L Frontal Lobe (-8, -20, 70)	-0.055	0.261	0.343	0.361	0.166	0.114	0.156	0.138	-0.539	-0.079	-0.006
		L Parietal Lobe (30, -44, 24)	0.315	0.167	0.259	0.256	0.074	-0.219	-0.046	0.013	0.188	0.091	0.479
	GM	*R Superior Frontal Gyrus (BA 6) (12, -22, 68)*	-0.064	0.158	0.102	0.201	-0.202	0.100	-0.092	0.239	-0.212	0.012	0.212
		R Cerebellar Vernis VIIB (2, -72, 32)	0.224	-0.093	0.074	-0.073	-0.303	-0.292	-0.202	-0.151	0.200	-0.317	0.176
		R Hippocampus (36, -10, -20)	-0.014	-0.140	-0.269	0.119	-0.317	-0.219	-0.385	-0.145	0.248	-0.409	-0.030
		R Precentral Gyrus (BA 6) (46, -9, 32)	-0.023	0.005	0.472	0.237	0.253	-0.150	0.046	0.025	-0.382	-0.171	0.030
		R Postcentral Gyrus (BA 43) (62, -8, 12)	-0.260	-0.312	-0.009	0.292	-0.023	-0.351	-0.147	-0.290	-0.224	-0.451	-0.236
sPTLD > HC	GM	*L Cerebellar Lobule III (4, -40, -18)*	0.467	0.605	0.210	0.109	0.385	0.787	0.433	0.026	0.067	0.071	0.071
			6 Month Follow-Up Visit										
RTH > HC	WM	*R Frontal Lobe (34, 32, 6)*	n/a	0.190	-0.235	0.269	0.288	0.140	0.220	0.474	0.406	0.067	0.321
	GM	*L Middle Frontal Gyrus (BA 6) (-28, 10, 58)*	n/a	0.550	0.154	0.061	-0.092	-0.152	0.128	**0.862****	0.345	0.400	0.429
sPTLD > HC	GM	*L Middle Frontal Gyrus (BA 6) (-30, 10, 62)*	n/a	-0.273	**-0.891****	-0.750	-0.582	-0.638	**-0.893****	-0.037	0.393	-0.657	-0.486

Fig. 4 Correlation matrix for ROI values and cognitive test scores. Shades of red = positive correlation direction; shades of blue = negative correlation direction. Correlations were run using Spearman's rank; significance is denoted by * <.05, ** < .01 if correlations also passed visual scatterplot inspection.

Discussion

This study examined brain changes associated with early, antibiotic-treated Lyme disease. Early elevated fMRI, including in white matter, activity was associated with RTH status. Much of the observed activity was located in the frontal and parietal lobes, consistent with brain regions previously shown to be relevant to this working memory task in healthy participants. [11, 22, 24, 35] Moreover, the intensity of early fMRI activity correlated with better health scores, as indicated by self-report. Robust brain activity, in or out of white matter, was not observed in those who developed sPTLD. Thus, early brain activity does not appear to be a pathology. Rather, it seems to reflect an adaptive healing response that leads to a favorable prognosis.

Although there was no pattern of association between brain activity and health status in the sPTLD group, an association between brain activity and cognition was observed. Specifically, at the follow-up visit, elevated brain activity correlated with reduced cognitive performance for processing speed, executive function, and attention. This is consistent with reports in the

literature of measurable cognitive impairments and subjective complaints of "brain fog" by PTLD patients.[7]

White matter activity during fMRI is unusual to observe due to this region's low energy demands, which are about only about 25% that of gray matter. [13, 36-38] White matter includes myelin and axons that interconnect gray matter regions. Synapses are formed in gray matter and most of the energy (delivered by the blood) is needed for brain metabolism there, such as to enable action potentials, restore ion gradients, and release neurotransmitters. Thus, detection of white matter activity via fMRI methods is uncommon but has been reported in healthy adults. [13, 14, 39, 40] We were struck, however, by the large degree of white matter activity observed at baseline, and that this observation was specific to the RTH group. Such activity was mitigated, but not fully resolved, six months post-treatment. In the sPTLD group, white matter activity was not observed at all. Taken together, these findings suggest that white matter activity is an important aspect of an adaptive response to *Bb* infection and that early, vigorous white matter activity is a harbinger of a healthy outcome. Our prior findings showed that people who developed PTLD can also elicit white matter activity. [11] In that study, white matter activity also corresponded to better health reports, suggesting that even in the PTLD stage, the brain continues to try to heal.

However, questions remain: what does this white matter activity represent, how is it detected via fMRI, and why does it relate to symptom severity and recovery in LD? Several clues can be gleaned from the data observed here. First, the time course of white matter activity generally correlated with that of gray matter activity. This indicates that energy metabolism, measured by proxy using the BOLD signal, was required by both brain matter types in a temporally dependent, synchronous way. Second, because axons and myelin do not have sufficient vascularization to support a BOLD signal, the BOLD signal observed here actually may have originated from a source surrounding the axon, which could not be disentangled visually with fMRI spatial resolution. Third, this phenomenon appears to be non-pathological because it corresponds to better, not worse, health outcomes.

The underlying mechanism that leads to white matter BOLD detection in this scenario should adhere to these qualities. A promising candidate mechanism may be mediated by astrocytes. Astrocytic proliferation is a response to neuronal damage and can be helpful or harmful, depending upon the context and duration. [41-44] Astrocytes assist action potential propagation at the Nodes of Ranvier (NR) along the myelin sheath. [45] Thus, if myelin were damaged or the NR altered in the course of LD, this could increase astrocytic involvement in the white

matter in an event-related (i.e., action potential) manner. This would correspond with concurrent astrocytic activity at the synapse in gray matter, where astrocytes use neurovascular coupling to help regulate blood flow needed for energy metabolism in an event-related manner. [46-48] These properties are consistent with the scenario of robust white matter activity correlating with healthy outcomes. Functional connectivity analyses in future studies could provide further insight into the interrelationship between white and gray matter networks.

An alternative interpretation is that neuroinflammation increased astrocytic metabolic demand, leading to secondary white matter BOLD activity that was neither adaptive nor compensatory. [49] This, too, could explain the mitigated response at six months after healing had occurred. However, if so, it is unclear why a similar pattern of white matter BOLD activity was not observed at either timepoint in the sPTLD group who presumably also experienced neuroinflammation.

While astrocytic involvement is plausible, this needs to be confirmed via direct astrocytic markers. Astrocytic reactivity can be measured in the cerebral spinal fluid (CSF) and blood serum by the protein glial fibrillary acidic protein (GFAP). Although GFAP levels were not obtained in the current study, increased GFAP levels were reported in patients with untreated LD long ago. [50] Notably, increases were detected within weeks of infection, decreased 4-8 weeks after antibiotic treatment, and correlated with duration of symptoms. This, too, fits with our pattern of findings. Future studies should examine the phenomenon of white matter activity in LD more pointedly, including additional measures that target white matter integrity (e.g., diffusion tensor methods), in combination with GFAP and other biomarkers, to better understand how brain activity relates to health outcomes.

White matter BOLD signal could also result from head motion or physiological noise during fMRI acquisition. In this study, image processing included motion correction to reduce this possibility. It is unlikely, however, that head motion would result in white matter BOLD signal revealed squarely within white matter tracts, in many cases > 90%, rather than along the edges of the brain or ventricle surfaces, as is often the case with head motion. It is also highly unlikely that motion artifacts occurred within one group at one timepoint only, with all other variables remaining constant (e.g., MRI scanner, scan sequence, analytic methods, etc.), and that the MRI values derived from these regions correlated with patient-reported health outcome scores, the latter being a replication of our prior findings in PTLD. [11] Nonetheless, white matter activity is an unusual finding and deserves to be interpreted with caution.

Dividing the LD group resulted in relatively small sample sizes for each subgroup. However, the robustness of activity observed in the RTH vs. HC comparison with only n=11 in the RTH group is impressive at $p < .001$. Small sample sizes likely masked group differences in direct comparison between the two LD subgroups, which were revealed when a slightly more liberal threshold of $p < .0025$ was applied. Larger-scale longitudinal studies are needed to confirm these findings. Because brain activations observed in the RTH group were reduced, but not entirely absent, by six months, participants should be followed longer than six months to identify if full resolution occurs.

In summary, this study demonstrated that an indicator of RTH status after *Bb* infection and treatment was early, robust brain activity located primarily in white matter. We postulate the source of white matter activity is related to astrocyte function, but this requires further investigation. Understanding how elevated white matter activity is related to RTH in those infected by *Bb* could aid early identification of those most vulnerable to developing PTLD and guide treatment.

Statements and Declarations

Funding

This study was funded by the PSquared Charitable Foundation.

Competing interests

The authors have no competing interests to declare that are relevant to the content of this article.

Ethics approval

This study was performed in line with the principles of the Declaration of Helsinki. Approval was granted by the Institutional Review Board of the Johns Hopkins University School of Medicine (IRB# 00212903).

Consent to participate

Informed consent was obtained from all individual participants included in the study.

Data availability

De-identified data not published within this article may be shared at the request of any qualified investigator for purposes of replicating procedures and results contingent upon approval of a data sharing agreement.

References

1. Marques A (2008) Chronic Lyme disease: a review. Infect Dis Clin North Am 22:341-360, vii-viii
2. Aucott JN (2015) Posttreatment Lyme disease syndrome. Infect Dis Clin North Am 29:309-323
3. Wormser GP, Dattwyler RJ, Shapiro ED, Halperin JJ, Steere AC, Klempner MS, Krause PJ, Bakken JS, Strle F, Stanek G, Bockenstedt L, Fish D, Dumler JS, Nadelman RB (2006) The clinical assessment, treatment, and prevention of lyme disease, human granulocytic anaplasmosis, and babesiosis: clinical practice guidelines by the Infectious Diseases Society of America. Clin Infect Dis 43:1089-1134
4. Arvikar SL, Crowley JT, Sulka KB, Steere AC (2017) Autoimmune Arthritides, Rheumatoid Arthritis, Psoriatic Arthritis, or Peripheral Spondyloarthritis Following Lyme Disease. Arthritis Rheumatol 69:194-202
5. Rebman AW, Bechtold KT, Yang T, Mihm EA, Soloski MJ, Novak CB, Aucott JN (2017) The Clinical, Symptom, and Quality-of-Life Characterization of a Well-Defined Group of Patients with Posttreatment Lyme Disease Syndrome. Front Med (Lausanne) 4:224
6. Rebman AW, Aucott JN (2020) Post-treatment Lyme Disease as a Model for Persistent Symptoms in Lyme Disease. Front Med (Lausanne) 7:57
7. Touradji P, Aucott JN, Yang T, Rebman AW, Bechtold KT (2019) Cognitive Decline in Post-treatment Lyme Disease Syndrome. Arch Clin Neuropsychol 34:455-465
8. Coughlin JM, Yang T, Rebman AW, Bechtold KT, Du Y, Mathews WB, Lesniak WG, Mihm EA, Frey SM, Marshall ES, Rosenthal HB, Reekie TA, Kassiou M, Dannals RF, Soloski MJ, Aucott JN, Pomper MG (2018) Imaging glial activation in patients with post-treatment Lyme disease symptoms: a pilot study using [(11)C]DPA-713 PET. J Neuroinflammation 15:346
9. Fallon BA, Keilp J, Prohovnik I, Heertum RV, Mann JJ (2003) Regional cerebral blood flow and cognitive deficits in chronic lyme disease. J Neuropsychiatry Clin Neurosci 15:326-332
10. Newberg A, Hassan A, Alavi A (2002) Cerebral metabolic changes associated with Lyme disease. Nucl Med Commun 23:773-777
11. Marvel CL, Alm KH, Bhattacharya D, Rebman AW, Bakker A, Morgan OP, Creighton JA, Kozero EA, Venkatesan A, Nadkarni PA, Aucott JN (2022) A multimodal neuroimaging study of brain abnormalities and clinical correlates in post treatment Lyme disease. PLoS One 17:e0271425
12. Gawryluk JR, Mazerolle EL, D'Arcy RC (2014) Does functional MRI detect activation in white matter? A review of emerging evidence, issues, and future directions. Front Neurosci 8:239
13. Gore JC, Li M, Gao Y, Wu T-L, Schilling KG, Huang Y, Mishra A, Newton AT, Rogers BP, Chen LM, Anderson AW, Ding Z (2019) Functional MRI and resting state connectivity in white matter - a mini-review. Magn Reson Imaging 63:1-11
14. Schilling KG, Li M, Rheault F, Gao Y, Cai L, Zhao Y, Xu L, Ding Z, Anderson AW, Landman BA, Gore JC (2023) Whole-brain, gray, and white matter time-locked

functional signal changes with simple tasks and model-free analysis. Proc Natl Acad Sci U S A 120:e2219666120

15. Aucott JN (2016) Slicestudies.org. In, Baltimore, MD

16. Ware JE, Jr., Sherbourne CD (1992) The MOS 36-item short-form health survey (SF-36). I. Conceptual framework and item selection. Med Care 30:473-483

17. Krupp LB, LaRocca NG, Muir-Nash J, Steinberg AD (1989) The fatigue severity scale. Application to patients with multiple sclerosis and systemic lupus erythematosus. Arch Neurol 46:1121-1123

18. Dworkin RH, Turk DC, Revicki DA, Harding G, Coyne KS, Peirce-Sandner S, Bhagwat D, Everton D, Burke LB, Cowan P, Farrar JT, Hertz S, Max MB, Rappaport BA, Melzack R (2009) Development and initial validation of an expanded and revised version of the Short-form McGill Pain Questionnaire (SF-MPQ-2). Pain 144:35-42

19. Beck A, Steer R, Brown G (1996) Beck Depression Inventory. The Psychological Corporation, San Antonio

20. Aucott JN, Yang T, Yoon I, Powell D, Geller SA, Rebman AW (2022) Risk of post-treatment Lyme disease in patients with ideally-treated early Lyme disease: A prospective cohort study. Int J Infect Dis 116:230-237

21. Aucott JN, Crowder LA, Kortte KB (2013) Development of a foundation for a case definition of post-treatment Lyme disease syndrome. Int J Infect Dis 17:e443-449

22. Marvel CL, Desmond JE (2012) From storage to manipulation: How the neural correlates of verbal working memory reflect varying demands on inner speech. Brain Lang 120:42-51

23. Marvel CL, Faulkner ML, Strain EC, Mintzer MZ, Desmond JE (2012) An fMRI investigation of cerebellar function during verbal working memory in methadone maintenance patients. Cerebellum 11:300-310

24. Berenbaum JG, Nadkarni PA, Marvel CL (2023) An fMRI analysis of verbal and non-verbal working memory in people with a past history of opioid dependence. Frontiers in Neuroscience 17

25. Chen SHA, Desmond JE (2005) Temporal dynamics of cerebro-cerebellar network recruitment during a cognitive task. Neuropsychologia 43:1227-1237

26. SPM12 (version 7771) Statistical Parametric Mapping In: https://www.fil.ion.ucl.ac.uk/spm/. Functional Imaging Laboratory Wellcome Centre for Human Neuroimaging

27. B M, JL A, R V, JB P (2002) Region of interest analysis using an SPM toolbox [abstract] Presented at the , June 2-6, 2002, . Available on CD-ROM in In: 8th International Conference on Functional Mapping of the Human Brain. NeuroImage, Sendai, Japan

28. Talairach J, Tournoux P (1988) Co-planar Stereotaxic atlas of the human brain 3-D proportional system, An approach to cerebral imaging. Thieme Medical Publishers, Inc., New York

29. Web BS In:

30. Schmahmann JD, Doyen J, Toga AW, Petrides M, Evans AC (2000) MRI Atlas of the Human Cerebellum. Academic Press, San Diego

31. Klein A, Andersson J, Ardekani BA, Ashburner J, Avants B, Chiang M-C, Christensen GE, Collins DL, Gee J, Hellier P, Song JH, Jenkinson M, Lepage C, Rueckert D, Thompson P, Vercauteren T, Woods RP, Mann JJ, Parsey RV (2009) Evaluation of 14 nonlinear deformation algorithms applied to human brain MRI registration. Neuroimage 46:786-802

32. Yushkevich PA, Avants BB, Pluta J, Das S, Minkoff D, Mechanic-Hamilton D, Glynn S, Pickup S, Liu W, Gee JC, Grossman M, Detre JA (2009) A high-resolution computational atlas of the human hippocampus from postmortem magnetic resonance imaging at 9.4 T. Neuroimage 44:385-398

33. Zhang Y, Brady M, Smith S (2001) Segmentation of brain MR images through a hidden Markov random field model and the expectation-maximization algorithm. IEEE Transactions on Medical Imaging 20:45-57

34. Eggert LD, Sommer J, Jansen A, Kircher T, Konrad C (2012) Accuracy and Reliability of Automated Gray Matter Segmentation Pathways on Real and Simulated Structural Magnetic Resonance Images of the Human Brain. PLOS ONE 7:e45081

35. Chen SH, Desmond JE (2005) Temporal dynamics of cerebro-cerebellar network recruitment during a cognitive task. Neuropsychologia 43:1227-1237

36. Logothetis NK (2003) The underpinnings of the BOLD functional magnetic resonance imaging signal. J Neurosci 23:3963-3971

37. Rostrup E, Law I, Blinkenberg M, Larsson HBW, Born AP, Holm S, Paulson OB (2000) Regional Differences in the CBF and BOLD Responses to Hypercapnia: A Combined PET and fMRI Study. Neuroimage 11:87-97

38. Harris JJ, Attwell D (2012) The Energetics of CNS White Matter. The Journal of Neuroscience 32:356

39. Gawryluk JR, Mazerolle EL, D'Arcy RCN (2014) Does functional MRI detect activation in white matter? A review of emerging evidence, issues, and future directions. Frontiers in neuroscience 8:239-239

40. Huang Y, Wei PH, Xu L, Chen D, Yang Y, Song W, Yi Y, Jia X, Wu G, Fan Q, Cui Z, Zhao G (2023) Intracranial electrophysiological and structural basis of BOLD functional connectivity in human brain white matter. Nat Commun 14:3414

41. Liddelow SA, Olsen ML, Sofroniew MV (2024) Reactive Astrocytes and Emerging Roles in Central Nervous System (CNS) Disorders. Cold Spring Harb Perspect Biol 16

42. Sofroniew MV (2015) Astrocyte barriers to neurotoxic inflammation. Nat Rev Neurosci 16:249-263

43. Jang E, Kim JH, Lee S, Kim JH, Seo JW, Jin M, Lee MG, Jang IS, Lee WH, Suk K (2013) Phenotypic polarization of activated astrocytes: the critical role of lipocalin-2 in the classical inflammatory activation of astrocytes. J Immunol 191:5204-5219

44. Liddelow SA, Guttenplan KA, Clarke LE, Bennett FC, Bohlen CJ, Schirmer L, Bennett ML, Munch AE, Chung WS, Peterson TC, Wilton DK, Frouin A, Napier BA, Panicker N, Kumar M, Buckwalter MS, Rowitch DH, Dawson VL, Dawson TM, Stevens B, Barres BA (2017) Neurotoxic reactive astrocytes are induced by activated microglia. Nature 541:481-487

45. Butt AM, Verkhratsky A (2022) Astrocytes regulate action potential propagation in myelinated axons: It is very crowded at the node of Ranvier. Cell Calcium 101:102518

46. Howarth C, Mishra A, Hall CN (2021) More than just summed neuronal activity: how multiple cell types shape the BOLD response. Philos Trans R Soc Lond B Biol Sci 376:20190630

47. Howarth C (2014) The contribution of astrocytes to the regulation of cerebral blood flow. Front Neurosci 8:103

48. Lia A, Di Spiezio A, Speggiorin M, Zonta M (2023) Two decades of astrocytes in neurovascular coupling. Front Netw Physiol 3:1162757

49. Virtuoso A, De Luca C, Korai SA, Papa M, Cirillo G (2023) Neuroinflammation and glial activation in the central nervous system: a metabolic perspective. Neural Regen Res 18:1025-1026

50. Dotevall L, Rosengren LE, Hagberg L (1996) Increased cerebrospinal fluid levels of glial fibrillary acidic protein (GFAp) in Lyme neuroborreliosis. Infection 24:125-129